

SIMON FRASER UNIVERSITY

# Blastomere Detection of Cleavage Stage Human Embryo

---

Course Project Report for ENSC 895

Weiguang Ding

301144137

[wding@sfu.ca](mailto:wding@sfu.ca)

## Table of Contents

Abstract .....	3
1 Introduction .....	3
2 Cell Boundary Detection .....	4
2.1 Frangi Vesselness Filter .....	4
2.2 Postprocessing .....	5
3 Blastomere Detection .....	6
3.1 Hough Transform .....	6
3.1.1 Hough Circle Transform .....	6
3.1.2 Boundary Orientation Used for Vote Reduction .....	7
3.2 Processing of Accumulator .....	7
3.2.1 Considering Different Radiuses .....	7
3.2.2 Considering Imperfect Circles .....	8
3.2.3 Find Possible Circles from the Accumulator .....	8
3.3 Verification of Circles .....	8
3.3.1 Verification Criteria .....	8
3.3.2 Verification Algorithm .....	9
3.4 Ellipse Fitting and Verification .....	9
3.4.1 Ellipse Fitting .....	9
3.4.2 Verification of Ellipse .....	10
4 Experiment and Evaluation .....	11
4.1 Evaluation of Boundary Detector .....	11
4.1.1 Evaluation Based on Ground Truth .....	11
4.1.2 Comparison between Ridge and Edge Detector .....	12
4.2 Threshold Setting for Boundary Detection .....	14
4.3 Evaluation of Cell Detection .....	14
4.3.1 Blastomere Detection Images .....	14
4.3.2 Statistics for Blastomere Detection .....	16
4.3.3 Analysis of Detection Results .....	17
5 Discussion and Future Work .....	18
Reference .....	19

## Abstract

In this course project, a method is proposed for blastomere detection and roughly localization in cleavage stage human embryo via image processing. Boundaries of blastomeres are first extracted by Hessian-based ridge detector followed by nonmaxima suppression and hysteresis thresholding. Based on the acquired boundaries, Hough circle transform is implemented to detect the presence of cell with consideration of boundary orientation. Then, screening algorithm is used to verify detected circles. Finally, the location of cells is approximated with circles and ellipses.

## 1 Introduction

In vitro fertilization (IVF) is a process by which female's egg cells are fertilized by sperm outside the body, in vitro. IVF belongs to assisted reproductive technology (ART), which is used in infertility treatments. In IVF procedure, retrieved oocytes are first fertilized and then are cultured for 1 to 5 days, after which 1 or more embryos will be transferred to the female's uterus. Embryos of the same patient differentiate in their qualities and development potentials. In order to improve the chance of positive pregnancy, these embryos must be inspected and only the top quality embryos with the highest normal growth potential should be transferred. The selection process is done manually and requires experts (such as reproductive endocrinologists and embryologist) to grade the embryos according to their morphologies and development patterns at different growth stages. This makes the IVF procedure expensive and selection procedure subjective.

Consequently, proposing solutions that decrease IVF's cost and/or improve the success rate are very desirable. This course project is proposed towards an automated embryo grading system which analyzes various aspects of embryos and their growth. The ultimate objective of the parent project is to improve the accuracy of healthy embryo selection procedure that ultimately leads to more success for the IVF procedure and lowering the overall cost associated with the manual intervention by the embryologists.

This course project aims to develop blastomere/cell detection, instead of shape description, technique for cleavage stage embryos. Boundaries of blastomeres are first extracted by Hessian-based ridge detector followed by nonmaxima suppression and hysteresis thresholding. Based on the acquired boundaries, Hough circle transform is implemented to roughly detect the presence of cell with consideration of boundary orientation. Then, screening algorithm is used to verify detected circles. Finally, the location of cells is approximated with circles and ellipses.

The rest of this report is organized as following: Section 2 will discuss the algorithm used for boundary detection. Section 3 will focus on blastomere detection using Hough transform. The algorithm is evaluated and analyzed in Section 4. Finally, Section 5 concludes this project and discusses future work.

## 2 Cell Boundary Detection

The embryo images used in this course project are acquired by Hoffman Modulation Contrast (HMC) [1] microscopes. The boundary of cells represent ‘ridge’ features instead of edge features, because the pixels around the boundary are darker. There is no significant difference between intensities inside and outside of cells. So, to extract cell boundary, a ‘ridge’ detector would be more desirable than an ‘edge’ detector. Comparison between ridge detector and edge detector will be done in section 4.

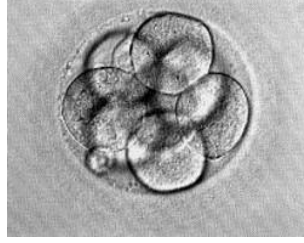


Figure 1: original embryo image

The Hessian-based Frangi Vesselness filter [2] is adopted to detect ridges in the image. Afterwards, it is combined with non-maximal suppression and hysteresis thresholding to extract one-pixel thick ridges. Finally, the small segments in the boundary image are removed.

### 2.1 Frangi Vesselness Filter

In the original work, the Frangi Vesselness filter is used for enhancement of blood vessels in Digital Subtraction Angiography images [2]. Here, it is used as ridge detector for boundary detection. The measure of ridge-likeness is based on the eigenvalues of hessian matrix of each pixel.

Consider the Taylor expansion of image  $I(x)$ , in the local neighborhood of point  $x_0$ :

$$I(x_0 + \delta x_0, \sigma) \approx I(x_0, \sigma) + \delta x_0^T \nabla_{0,\sigma} + \delta x_0^T H_{0,\sigma} \delta x_0 \quad (1)$$

$H_{0,\sigma}$  is the hessian matrix computed in  $x_0$  with scale  $\sigma$ . For 2D image, the hessian matrix  $H_{0,\sigma}$  has two eigenvectors  $\lambda_1$  and  $\lambda_2$ ,  $|\lambda_1| \leq |\lambda_2|$ .

The “blobness measure” is defined as

$$R_B = \lambda_1 / \lambda_2 \quad (2)$$

The ratio of eigenvalues measures the ratio of change rates along two vertical directions. If the blobness measure is large, the change rates between two directions are close. Consequently, the blobness is large and the neighborhood of the corresponding pixel is more “blob-like”. If the

blobness measure is small, the difference between change rates would be large. Consequently, the neighborhood of the corresponding pixel is more “line-like”.

The “second order structureness” is defined as

$$S = \|H\|_F = \sqrt{\lambda_1^2 + \lambda_2^2} \quad (3)$$

Having large hessian eigenvalues represents there is large value changes around the given pixel. Consequently, larger second order structureness represents that the pixel contains more structure information.

The “vessel likeliness measure” at a certain scale is defined as

$$V_0(\sigma) = \begin{cases} 0 & \text{if } \lambda_2 > 0, \\ \exp\left(-\frac{R_B^2}{2\alpha^2}\right) \left(1 - \exp\left(-\frac{S^2}{2\beta^2}\right)\right) & \text{otherwise} \end{cases} \quad (4)$$

Here,  $\alpha$  and  $\beta$  are parameters which are used to control the scale of “blobness measure”  $R_B$  and the “second order structureness”  $S$ .  $\sigma$  is the scale of used for detect ridges. Large scale represents wide ridge.

$V_0(\sigma)$  increases with the decrease of  $R_B$  and the increase of  $S$ , which means small blobness measure and large second order structureness give large vessel likeliness measure.

The vessel likeliness function would be maximized at the scale which corresponds to the size of ridge. Therefore, it is calculated over different scales, and the largest value of  $V_0$  will be considered as the vessel likeliness at that point.

$$V_0 = \max_{\sigma_{\min} \leq \sigma \leq \sigma_{\max}} V_0(\sigma) \quad (5)$$

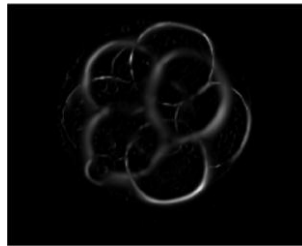


Figure 2: vesselness filtered embryo image

## 2.2 Postprocessing

After acquiring the vessel likeliness function  $V_0(x)$  over the image, nonmaxima suppression and hysteresis thresholding is performed in the same manner as canny edge detector [3]. Then, small segments are removed from the edge image.

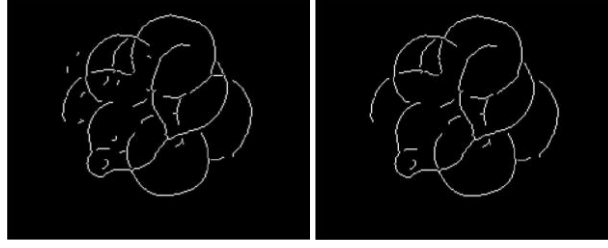


Figure 3: the left image is the detected boundaries after nonmaxima suppression and hysteresis thresholding, the right one is after small segments removal

### 3 Blastomere Detection

After the one-pixel thick boundary of cell is obtained, circles need to be found out of the boundary image. In the boundary image of cleavage embryo, cells have different situations including imperfect circles, partial boundary, largely overlapping and etc. All these characteristics require that the detection approach to be robust with interference from boundary of other cells and the incompleteness of cell boundary itself.

The Hough transform scheme is adopted for circle detection [3]. The accumulator of Hough transform is accumulated over 3D space. Possible circle candidates are found out of the local maximum points in this accumulator. Afterwards, screening algorithm is developed based on the circle properties. Finally, the remaining circles are fitted as ellipses and screening with respect to the property of ellipse is used to eliminate false detection.

#### 3.1 Hough Transform

##### 3.1.1 Hough Circle Transform

The equation for 2D circle is

$$(x - x_c)^2 + (y - y_c)^2 = r^2 \quad (6)$$

For a given radius  $r$ , every point in the boundary image corresponds to a circle in the parameter space  $x_c, y_c$ . With certain range of the radius  $r_{\min} \leq r \leq r_{\max}$ , parameters  $r, x_c, y_c$  form a 3D parameter space. By accumulating circles in of different radiuses in the parameter space for each pixel in the boundary image, the 3D accumulator is formed with each point in it represents the likelihood of the presence circle at that point. In other words, if the value of one point in the accumulator  $v(x_{c0}, y_{c0}, r_0)$  is large, it means the probability of the presence of circle centered in  $(x_{c0}, y_{c0})$  and with the radius  $r_0$  is large.

### 3.1.2 Boundary Orientation Used for Vote Reduction

Every pixel on the boundary belongs to only one circle. However, by the conventional Hough transform, every point will correspond to a set of circle with different radiuses in the parameter space. Most pixels on these circles are redundant. What is worse, they bring significant noise to the following processing. To deal with this problem in circle detection, boundary orientation information needs to be used.

Orientation of the eigenvector of Hessian matrix is used as the orientation of boundaries. The boundary orientation is considered in a similar manner with previous work [4]. In this work, Sobel operator was used to get the edge orientation. In our case, boundaries are detected by calculation of their hessian eigenvalues. Consequently, eigenvector of Hessian matrix is used to represent the orientation of boundaries.

Knowing the orientation of the boundary, circles in parameter space are cropped to only two pieces of arcs, which lie on the small range at the end of radius which is perpendicular to the boundary orientation.

One remaining problem is that even the boundary orientation information is used, there are still two pieces of arcs and only one of them is useful. Coping with this problem, orientation information in the neighboring boundary pixels are used for determining the direction of curvature in the given boundary pixel.

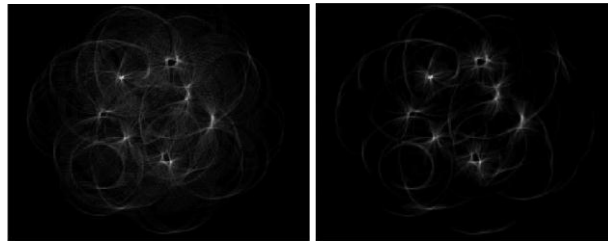


Figure 4: The left image is the parameter space  $x_c, y_c$  with a given radius without consideration of boundary orientation. The right image is the one considering orientation of boundary. It is clearly that the right image has less “noise” than the left one.

## 3.2 Processing of Accumulator

### 3.2.1 Considering Different Radiuses

The criterion for determination of the presence circle is the ratio of number of accumulated pixels and the pixel number of a full circle. For circles with different radiuses, the pixel numbers of full circle differ. And this was not considered in the previous acquired accumulator.

For normalization of points in parameter space with different radiuses, the value for each point is divided by the perimeter of circle with corresponding radius.

### 3.2.2 Considering Imperfect Circles

The blastomeres in embryo are rarely perfect circle, so tolerance of the vote position need to be considered. This is done by filtering the accumulator. For every point in different  $x_c, y_c$  parameter planes, the value is recalculated by a Gaussian shape filter with the center value equals to 1. By doing this, radius variations for a single non-circular cell are considered.

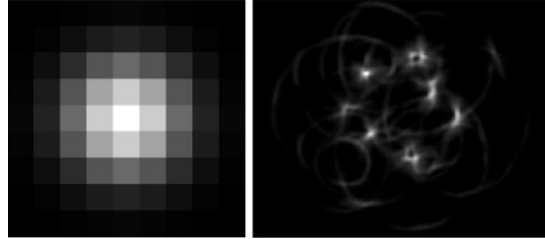


Figure 5: the left is  $9 \times 9$  Gaussian filter used with center equals to 1. The right image is the filtered parameter space  $x_c, y_c$  with a given radius

### 3.3.3 Find Possible Circles from the Accumulator

In this step, possible circles are founded based on the 3D parameter accumulator. Points with large values in parameter accumulator represent large likelihood of circles with corresponding parameters. The procedure is described as follows.

First, a threshold for determine the presence of circle is initialized. For every point in parameter space, if the value is above threshold and is the maximum in a certain 3D neighborhood, this point is considered as a circle candidate. If too few circles are found under the initial threshold, a lower threshold would be used. Until the number of circle candidates meet the requirement for further circle selections. The figure below shows the first 20 detected circles.

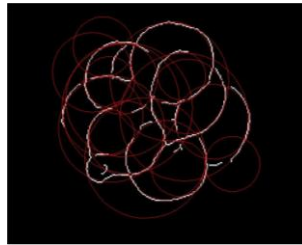


Figure 6: first 20 detected circles

## 3.3 Verification of Circles

Large amount of circles would be found in previous step. Now, invalid circles need to be screened out by the property of the fitted circle and their relationship.

### 3.3.1 Verification Criteria

Three criteria are used for screening out invalid circles.



First, if a circle has part out of the image, it would be considered invalid. This is obvious embryos are fully contained inside the image for all images of our dataset. Second, if the radius of one circle is very different from other circles, it is invalid. Third, for largely overlapping circles with different radiuses, the one with the radius similar to other verified circles should be chosen and other circles need to be eliminated.

### 3.3.2 Verification Algorithm

The algorithm is stated as follows.

The first two detected circles in previous step are labeled as valid.

For the each of the following circle, if the circle has part out of image, or if the radius of it is out of the radius range defined by mean and variance of previous verified circles. This circle is marked as invalid.

If the circle pass the above 2 examinations, and is not largely overlapped with other verified circles, it is considered as a valid circle.

If the circle is largely overlapped with existing verified circle, the one with the more similar radius with the rest circles would be chosen as the valid one. The measure of similarity is the variance of the radius of given circle and the radiuses of rest circles.

If  $n$  consecutive previous detected circles are invalid, the algorithm stops examining following ones.

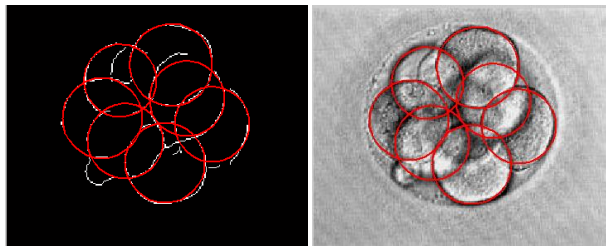


**Figure 7:** The left image is the verified circles over-imposed on the boundary image. The right image is the verified circles over-imposed on the original embryo image.

## 3.4 Ellipse Fitting and Verification

Ellipse is better shape descriptor than circle, although the focus of this project is detection instead of shape description. In this section, ellipses are fitted based on the detected circles. Furthermore, the fitted ellipse parameters are used to verification of detection.

### 3.4.1 Ellipse Fitting

The fitting algorithm is stated as follows.

For every detected circle, choose the a ring area with radiuses  $r - \sigma$  and  $r + \sigma$ . And use the boundary pixels inside this area for further ellipse fitting.

Then, “boundary cleaning” based on boundary orientation is performed. Each ring area will contain boundary pixels coming from different cells, and this would lead to large errors of the following ellipse fitting. So, “boundary cleaning” is necessary. Here, the cleaning is based on the direction with boundary pixels which is based on the orientation of the eigenvector of Hessian matrix. A valid range is defined for every boundary pixel by orientation of the line segment between that boundary pixel and the given circle center. So, only boundary pixels with similar orientation with the corresponding concentric circle are preserved.

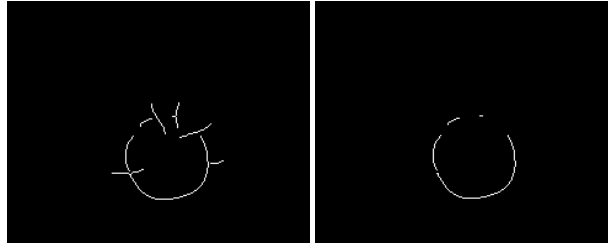


Figure 8: The left image is the boundary pixels inside a certain “ring”. The right image is the result after “cleaning” using boundary orientation information.

After boundary cleaning, the direct least square ellipse fitting [5] is adopted for ellipse fitting.

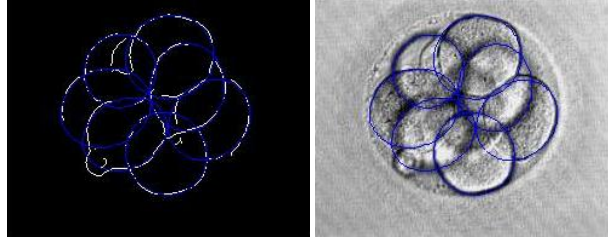


Figure 9: The left image is the fitted ellipses over-imposed on the boundary image. The right image is the fitted ellipses over-imposed on the original embryo image.

### 3.4.2 Verification of Ellipse

For some embryo images, the blastomeres are deformed because of the pressure between cells. For this type of embryos, their blastomeres are usually more ellipse-like and will result in multiple circles detected for single blastomere.

To eliminate this effect, ellipses is fitted to every detected blastomeres based on circle detection. And then, verification based on ellipse fitting is used for the second-round screening.

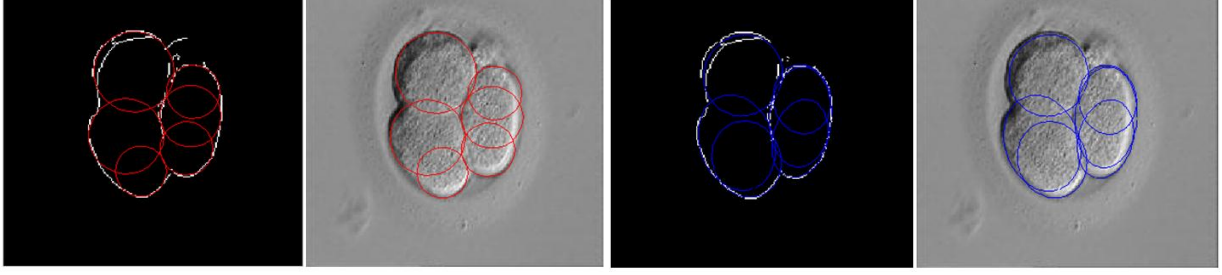


Figure 10: example of multiple detections for single blastomere

In this stage, largely overlapping is eliminated. Similar to the verification of circles which is based on the variance of radiuses, the ellipse verification is based on the variance of areas. In other words, if several ellipses are largely overlapped, area of each one of them will be compared with other ellipses. The measure of similarity is the variance of the area of given ellipse and the areas of rest ellipses which are not involved in the comparison.

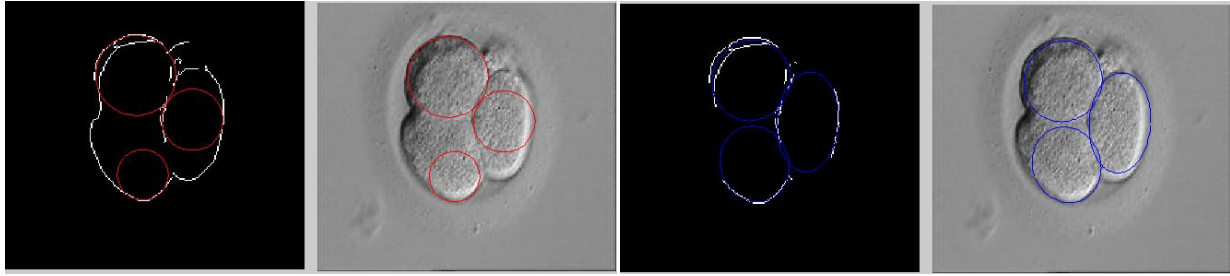


Figure 11: previous embryo image after ellipse verification

## 4 Experiment and Evaluation

32 images collected from internet are used for analysis and evaluation of the detection algorithm.

### 4.1 Evaluation of Boundary Detector

For objective evaluation of the boundary detector performance, the detected boundaries need to be compared with the manually labeled ground boundaries. By this comparison, statistics like false alarm rate, misdetection rate, recall, precision and F-measure is acquired for evaluation of the boundary detector.

#### 4.1.1 Evaluation Based on Ground Truth

Here, the edge assignment algorithm [6] is adopted for comparing ground truth detected boundaries. In this algorithm, one-to-one association between ground truth and detected edge pixels is established by minimizing a distance cost function.

By implementing this algorithm, number of true positive, false positive (false alarm) and false negative (misdetection) can be acquired. Here, true positive means that a given ground truth

boundary pixel is detected by the detector. False positive means that a detected boundary pixel has no corresponding ground truth boundary pixel. False negative, or misdetection, means a ground truth boundary pixel is not detected by the detector.

Using these statistics, the precision, recall and F-measure can be obtained from the following formula.

$$precision = \frac{TP}{TP+FP} \quad (7)$$

$$recall = \frac{TP}{TP+FN} \quad (8)$$

$$F - measure = (1 + \beta^2) \frac{precision \cdot recall}{\beta^2 \cdot precision + recall} \quad (9)$$

Here, precision represents the correction rate in detected boundary pixels. Recall represents the detected boundary pixels in the ground truth pixels. F-measure is the harmonic mean of precision and recall and is used as the overall measure of the detector performance. In this project, it is always  $\beta = 1$ . In this case,

$$F - measure = \frac{2TP}{2TP+FP+FN} \quad (10)$$

#### 4.1.2 Comparison between Ridge and Edge Detector

For boundary detection, two different types of detectors are available, ridge detectors and edge detectors. In this section, these two detectors are compared based on the statistical measures precision, recall and F-measure. Best performance of each detector is shown. The reason for choosing ridge detector is stated.

The edge detector used here is the well-know canny edge detector. It is based on the gradient values of embryo image.

The ridge detector is the Frangi vesselness filter combined with ‘canny-like’ post processing, namely, nonmaxima suppression and hysteresis thresholding. As mentioned previously, it is based on eigenvalues of hessian matrix.

Following analysis is based on the statistic property of embryo image shown in Figure 1. The threshold value here is the higher threshold value for hysteresis thresholding, and the lower threshold value is set to be 0.4 times the higher threshold.

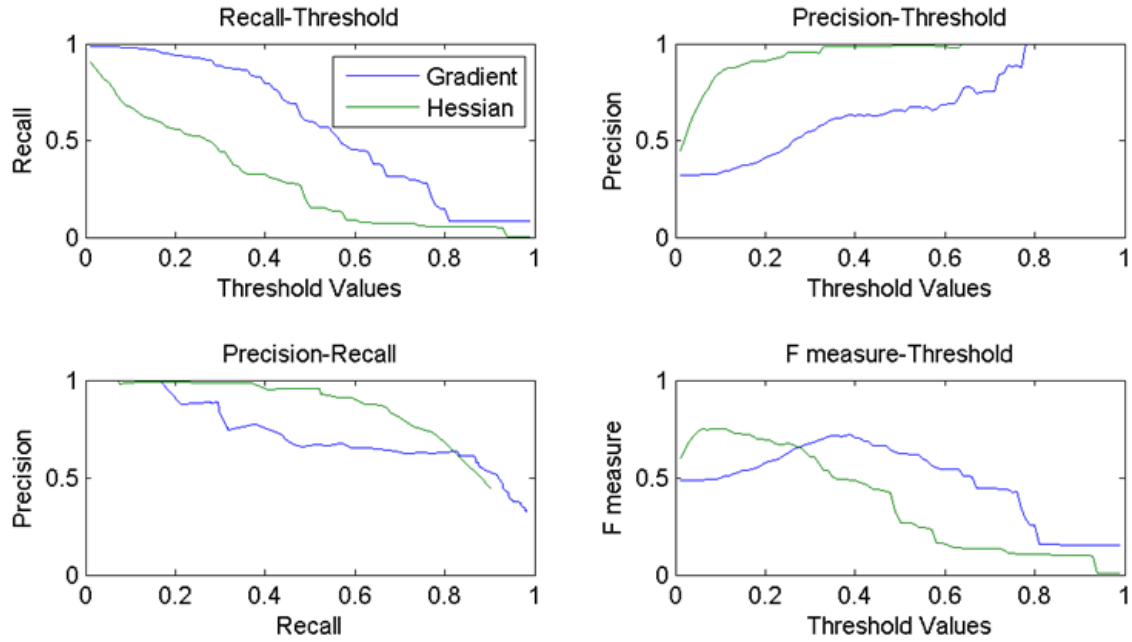


Figure 12: the statistics curve for the embryo image in Figure 1

Recall-Threshold, Precision-Threshold, Precision-Recall, and Fmeasure-Threshold curves are shown in above figure. We can see that edge detector in general has higher recall and the ridge detector has higher precision. This means that the ridge detector will found less boundary pixels, but the for the detected boundary pixels, they are highly possible to be true edges. The F-measure represents a single measure for the boundary detection result over the domain of threshold values from 0 to 1.

Next, the threshold values corresponding to the largest F-measure for these two detectors are chosen respectively as the optimal thresholds.

Ground Truth Boundary Edge with Optimal Threshold Ridge with Optimal Threshold



Figure 13: boundary detection results with optimal threshold. The left image is the ground truth, middle one is the edge detection, and the right one is the ridge detection

From the above shown boundary detection results, we can found that edge detection usually give double edges for single blastomere boundary. Also, the shapes of some cells are not preserved, for example the blastomere at 7 o'clock direction.

Based on the observation of “best” results of both edge and ridge detections over the dataset, the ridge detector is adopted as the boundary detector for blastomere detection.

## 4.2 Threshold Setting for Boundary Detection

Continued with the last section 4.1, the Fmeasure-threshold curves are used for selection of ridge detector threshold.

For the first 16 images, their Fmeasure-threshold curves are summed up to form a “total” Fmeasure-threshold curve. The threshold value which corresponds to the maximum F-measure is selected as the optimal threshold for this dataset. Then this threshold is also used for these other images, and there is no observable difference between these 2 sets of images. So, in the following analysis, these 2 sets of images are not distinguished.

## 4.3 Evaluation of Cell Detection

In this project, whether detection is correct and whether a blastomere is detected is judged manually.

### 4.3.1 Blastomere Detection Images

Detection results for 32 embryo images are shown as follows. Circles and ellipses are over-imposed on original cleavage embryo images.

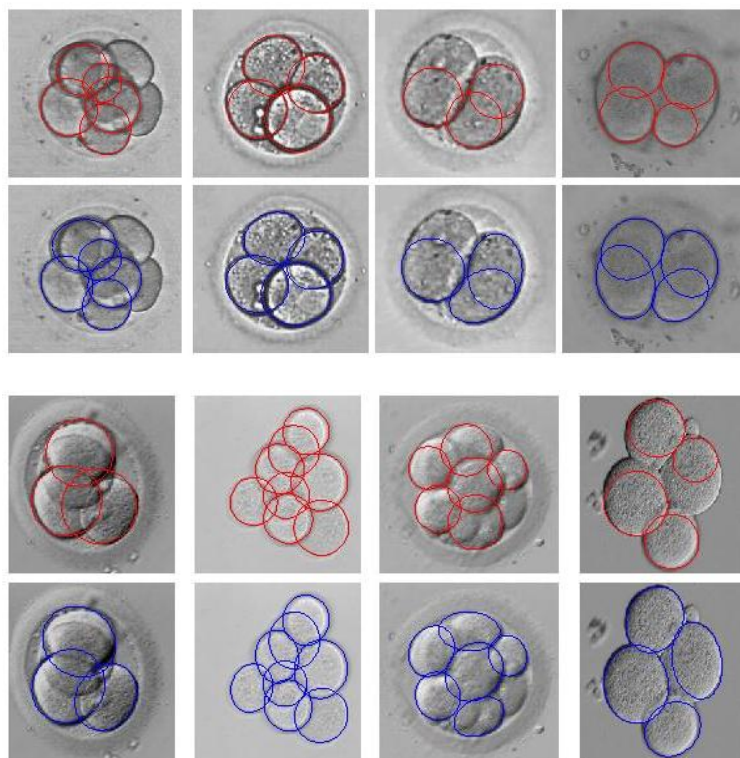


Figure 14: Over-imposed circles and ellipses on original embryo images



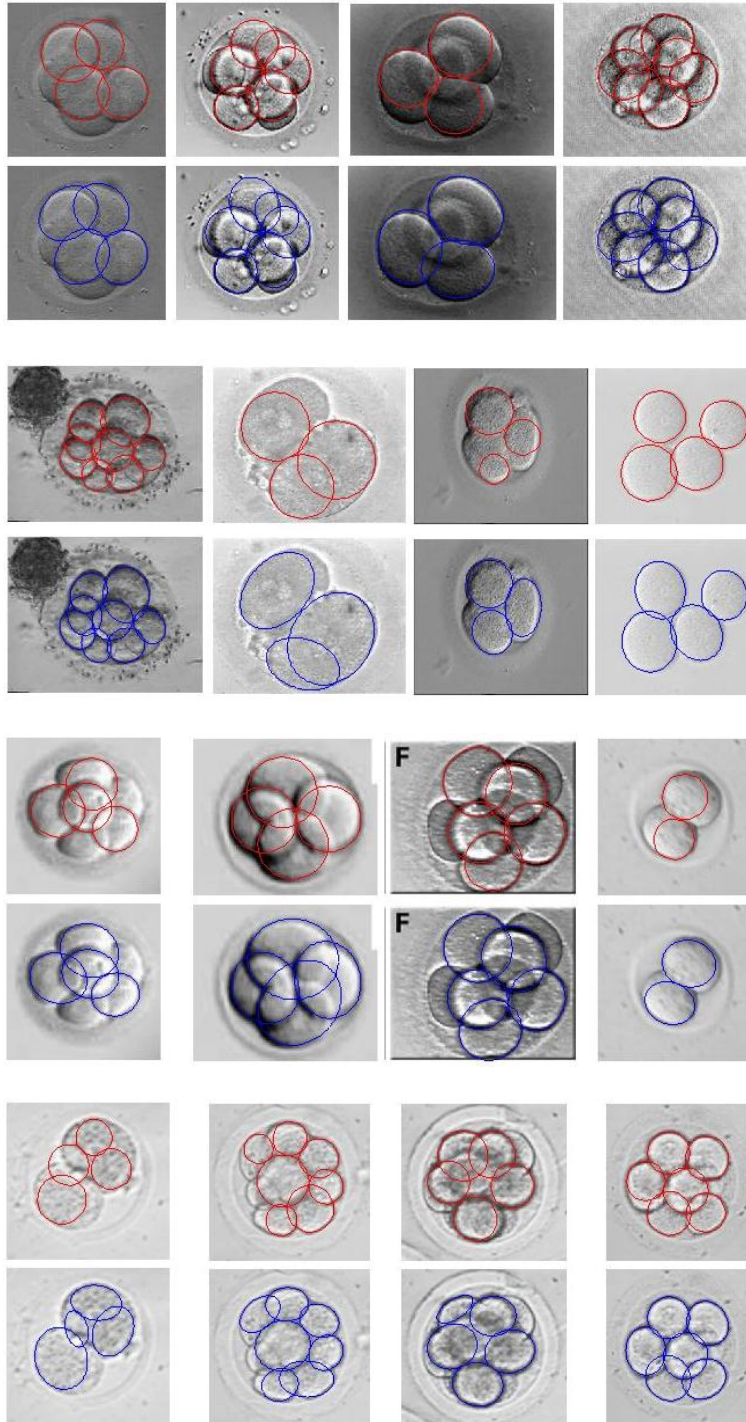


Figure 15: Over-imposed circles and ellipses on original embryo images continued

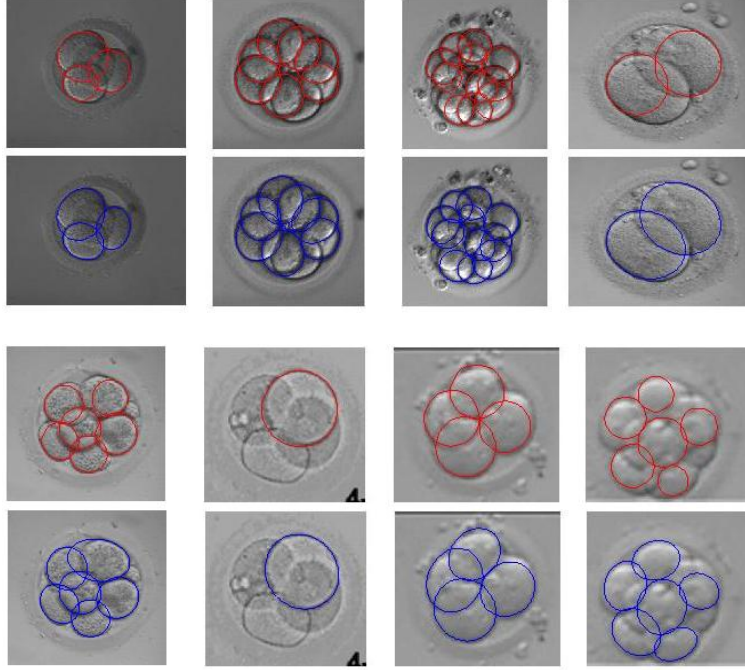


Figure 16: Over-imposed circles and ellipses on original embryo images continued

#### 4.3.2 Statistics for Blastomere Detection

In this section, the performance of the detection algorithm is analyzed statistically.

In these 32 embryo images, there are totally 176 blastomeres and 152 cells detected. Among them, 136 are correct detections.

Here, we define true positive (TP) as the correct detection, false alarm/false positive (FP) as the detected circle/ellipses which are not correspond to any real cell, misdetection/false negative (FN) as the real cells that are not detected. Afterwards, the precision and recall are again used to measure the performance after they first appeared at section 4.1.1.

The total precision for all blastomere is 0.8947. This means for a given detection, the probability that it is correct detection is 0.8947. The total recall is 0.7727, which means for a given real cell, the probability that it will be correctly detected is 0.7727.

The average precision is 0.8755, which means the average for the precisions of all embryo images. Similarly, the average recall is 0.7562.

The scatter points in Precision-Recall space which represent different embryo images are shown as the figure below. Due to overlapping, there are less than 32 points.



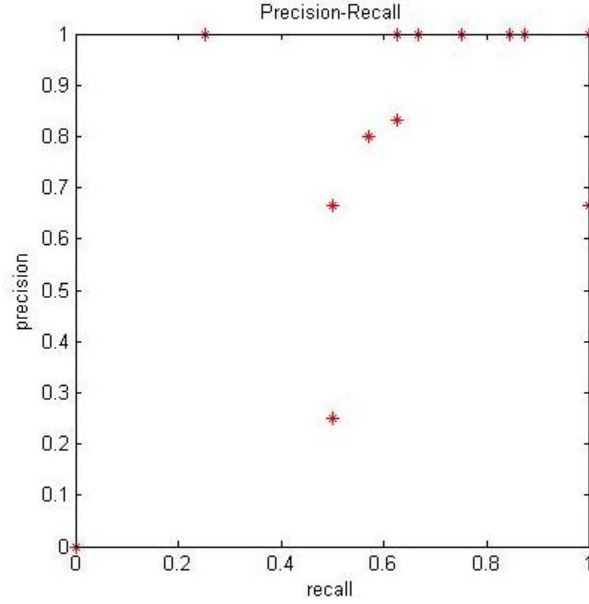


Figure 17: detection results in Precision-Recall space

#### 4.3.3 Analysis of Detection Results

Images used in this project are collected from internet, and this makes the dataset diverse. In this section, different kinds of detection failures are analyzed.

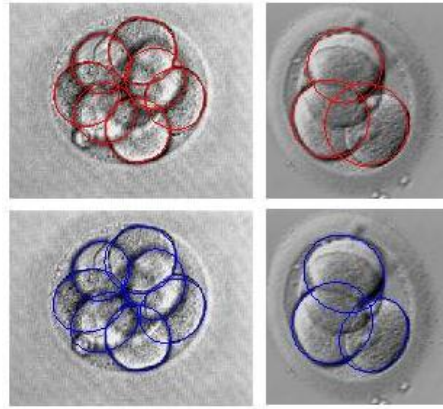
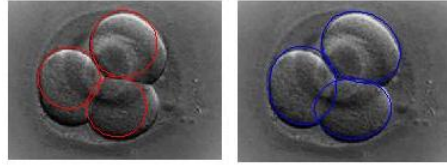


Figure 18

Figure: failure because of edge feature instead of ridge feature

The boundary detection of proposed detection approach is based on ridge detectors. If the cell is dark area in the image, the ridge detector would fail to detect the boundary. From the above images, we can see dark areas in the middle of each embryo respectively. This is rather edge features, and ridge detector is not suitable for it.



**Figure 19: failure because of high boundary threshold**



**Figure 18: the left image is the boundary detection with the optimal threshold for this image. The right image is the boundary with the threshold for the dataset.**

The threshold for boundary detection is set by optimization over a set of images, so it might be improper for single image. From the above images, we can find the reason of failure detection of the middle embryo is the improper threshold.

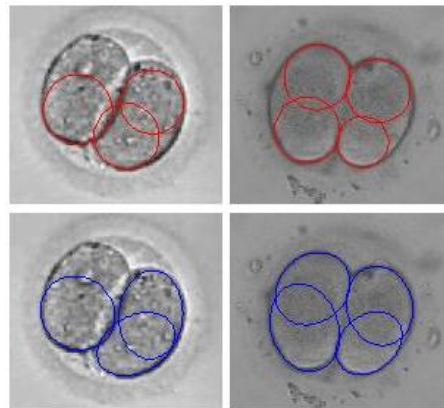


**Figure 19: failure because of non-circular shape**

This detection algorithm is based on Hough circle transform, and this requires that the blastomeres to be nearly circular. If the cell shape is far from circle, multiple detections for single cell might happen.

## 5 Discussion and Future Work

This course project provides an algorithm for cell detection in cleavage stage human embryos. Frangi vesselness filter is combined with nonmaxima suppression and hysteresis thresholding for boundary detection. Hough circle transform followed by circle verification is performed for blastomere detection. Finally, ellipses are fitted to detected circles and ellipse property is used for detection verification.

The boundary of detection has been evaluated in an objective manner, which is done by comparison between detected boundaries and the ground truth boundaries. However, for the circle detection part, the evaluation is done manually by judging whether the detected circles are able to represent the blastomeres. In the future, the evaluation will be done by comparison between manually labeled ground truths and detected blastomeres by given objective criteria. In this manner, parameters can be trained automatically to get the optimal detection result.

The dataset used in this course project is collected from internet, so there are variations among those images. Effort has been done for grouping different image types and qualities according to which the parameters can be set separately. However, maybe due to the small amount of data, this trial is not successful. After getting images from our collaborating clinics, which are expected to be the same type and have high quality, parameters will be set more accurately and the better performance of the algorithm is highly hopeful.

For the failures mentioned in the previous section, future improvement can be made. For detection of cell which is shown as dark area, edge detector might be incorporated into the current scheme to detect edge features. For thresholding problem, automatic threshold selection approach needs to be considered. For non-circular shape cell detection, techniques other than Hough transform might need to be studied.

This course project aims to develop technique for detection of blastomeres. For our future work, shape description would be performed after the detection stage. More accurate model would be used instead of circle or ellipse. The blastomere detection could be considered as an initialization of the shape description algorithm.

## Reference

- [1] R. Hoffman, L. Gross, Modulation contrast microscope, Appl. Opt.14, 1975, pp. 1169–1176
- [2] A. F. Frangi, W. J. Niessen, K. L. Vincken, and M. A. Viergever, Multiscale vessel enhancement filtering, Medical Image Computing and Computer-Assisted Interventions—MICCAI’98, pp. 130–137
- [3] Gonzalez R, Woods R: Digital Image Processing, 2nd edition. New Jersey, Prentice Hall; 2002.
- [4] C. Kimme, D. Ballard and J. Sklansky, Finding circles by an array of accumulators. Comm. Assoc. Comput. Mach. 18 (1975), pp. 120–122
- [5] A. Fitzgibbon, M. Pilu, and R. B. Fisher, Direct least square fitting of ellipses, IEEE Trans. Pattern Anal. Machine Intell., vol. 21, pp. 477–480, May 1999.
- [6] G. Liu and R. M. Haralick, Assignment problem in edge detector performance evaluation, Comput. Vision Pattern Recognit. 1 (2000), pp. 26–31.